High-T_c Superconducting Membrane: (II) Nanosized Superconducting Particles into α-Alumina Support

Joo-Byoung Yoon, Eue-Soon Jang, Soon-Jae Kwon, Andre Ayral,† Louis Cot,† and Jin-Ho Choy*

National Nanohybrid Materials Laboratory, School of Chemistry & Molecular Engineering, Seoul National University, Seoul 151-747, Korea
†Laboratoire de Matériaux et Procédés Membranaires(LMPM), ENSCM, 8 Rue de l'Ecole Normale, F34296, Montpellier, France
Received December 8, 2000

Porous superconducting membranes were realized by the electrophoretic deposition of bismuth cuprate colloid precursors. In order to prepare superconducting colloidal suspension, the high T_c bismuth cuprate superconductor, $Bi_2Sr_2CaCu_2O_{8+y}$ or $Bi_2Sr_2Ca_2Cu_3O_{10+y}$, should first be intercalated with mercury iodide molecules and subsequently with organic compounds such as pyridine and alkylpyridinium to induce interlayer complexes like bis(alkylpyridinium)tetraiodomercury and bis(Py)diiodomercury. Finally, the resulting organic complex intercalates were dispersed in an organic solvent to form superconducting colloids with an average particle size of ~200 nm. Gas separation membranes were prepared by the filtration of superconducting nano particles through an a-alumina support. Their physical properties such as superconductance, porosity and pore size were measured by SQUID and mercury porosimetry, respectively, and their morphology and thickness were checked by SEM. The gas permeation experiments for nitrogen and oxygen mixture were performed at liquid nitrogen temperature.

Keywords : Gas separation, Superconducting membrane, Superconducting colloid.

Introduction

Inorganic membranes have long been studied as useful materials for separation, purification and catalytic reaction and have become extremely attractive as alternatives to polymer membranes due to their pertinent thermal and chemical stability and durability. Ceramic filter and percolation materials using simple ceramics have been applied in industry for several decades. Nowadays highly efficient and multi-functional membranes using various nanocomposites of inorganic/organic, inorganic/inorganic, and inorganic/polymer have become prominent and their fields of application have enlarged to include environment, medical science, pharmaceuticals, and biology, etc.[1]

Inorganic membranes for gas separation have been widely studied for their potential industrial applications. Since the separating principle is mainly based on the shape selectivity of the porous dimensions of membranes, the pore size control of porous materials has been a major topic of research interest. Although a partial success was achieved in separating relatively large gas or solvent molecules from mixtures of different size, it was realized that molecules of similar size like N_2/O_2 mixed gas could scarcely be separated simply by using the porous membrane only since the size difference between N_2 (3.64 Å) and O_2 (3.46 Å) is negligible, as shown in Table 1.[2] Therefore, it is of great importance to develop a new porous membrane material for separating such gas molecules based on the differences in physical properties.

Recently, attempts have been made to develop new membranes based on the different chemical or physical properties of membrane materials. Polyaniline or polyaramide membranes are examples of gas separation membranes using the chemical property of macromolecules whereby they have greater affinity toward oxygen than to nitrogen molecules.[3] In general, the oxygen/nitrogen selectivity is often greater than 6 in polymer membranes, which are, however, fairly low in permeability. Even though some permeable polymers with a particular selectivity have recently been suggested, no better material has been developed beyond the upper bound of permeability square selectivity.[4] On the other hand, the physical properties of membrane materials have been intensively studied. These include the molecular pumping character of perovskite[5] and alkali metals.[6] The former is based on oxygen ionic conductivity, and the oxygen/nitrogen separation factor often reaches to infinity, while the latter uses the quadruple moment difference between oxygen and nitrogen; however, such membranes would suffer from low permeation or low selectivity.

Superconducting and ferromagnetic membranes are further examples of the use of the physical properties of membrane materials. The former could be applied to gas separation using the diamagnetic property of superconducting membranes below the critical temperature (T_c), which means that the permeation of diamagnetic nitrogen molecules is preferable to that of paramagnetic oxygen molecules.[7] However, it is difficult to make a microporous superconductor membrane with a pore size below 10 Å and the theoretical result derived from the mirror principle is inadequate for gas

*To whom all correspondence should be addressed. Tel: +82-2-880-6658, Fax: +82-2-872-9864, e-mail: jhchoy@plaza.snu.ac.kr

Table 1. Physical properties of various gas molecules

molecule	magnetic property at boiling point [χ_m (10^{-6} cm^3/mol)]	boiling point (K)	kinetic diameter (Å)
oxygen (O_2)	paramagnetic (+3402 for gas) paramagnetic (+7667 for liquid)	90.1	3.46
nitrogen (N_2)	diamagnetic (–12.05)	77.4	3.64
argon (Ar)	diamagnetic (–6.99)	87.3	3.35
Nitric oxide (NO)	paramagnetic (+1461)	121.4	~3.8
carbon dioxide (CO_2)	diamagnetic (–20)	194.7	~4.0

separation.[8] If one examines the formalism of the mirror principle carefully, it is easily determined that the grain size resulting from diamagnetic and paramagnetic interaction is too small to be utilized for gas separation. Ferromagnetic gauze was also used in gas separation of paramagnetic and diamagnetic molecules,[9] but it needs a strong magnetic field to induce a high selectivity. Moreover, in the case of a 10 T magnetic field produced by a superconducting magnet, the (O_2/N_2) selectivity did not exceed 2. The magnetic field gradient concept was suggested as a means of separating paramagnetic oxygen and diamagnetic argon through superconducting membrane, where the field gradient in the vicinity of the pore window is the highest. Therefore, oxygen molecules could permeate better than diamagnetic nitrogen molecules.[10] They also calculated the theoretical magnetic force for oxygen molecules induced by the Meissner effect of a superconductor. A good model membrane, which considers the geometrical shape, applied field strength and pore size, was postulated and YBCO was suggested as the superconducting filter for separation of nitrogen and oxygen.[11-12]

In this study, primary attention has been devoted to the development of a new porous superconducting membrane resulting in the facile preparation of electrophoretic deposition from bismuth cuprate colloids in order to separate O_2 molecules selectively from the $N_2 + O_2$ mixed gas.

Experimental Procedure

Preparation of superconductor. Polycrystalline samples of Bi2212 and (Bi,Pb)2223 were prepared by conventional solid state reaction. At first, the powder reagents of Bi_2O_3, PbO, $SrCO_3$, $CaCO_3$ and CuO were thoroughly mixed with molar ratios of Bi : Sr : Ca : Cu = 2 : 1.5 : 1.5 : 2 for Bi2212 and Bi : Pb : Sr : Ca : Cu = 1.85 : 0.25 : 2 : 2 : 3 for (Bi,Pb)2223, respectively. The mixtures obtained were calcined at 800 °C for 12 hours in air, and then the pre-fired materials were pressed into 10 mm disk-shape pellets by a pressure of 5 ton/cm^2 and finally sintered with intermittent grindings. The single-phase samples of Bi2212 and (Bi,Pb) 2223 were prepared by heating in air at 845 °C for 48 hours and at 850 °C for 130 hours, respectively.

Preparation of HgI_2-intercalation and organic intercalation complexes. The intercalation of HgI_2 was performed by heating the vacuum-sealed tube containing the pristine $Bi_2Sr_2Ca_1Cu_2O_y$ with five equivalent HgI_2 and 0.2 molar iodine per formula unit of the host superconductor. While the first staged HgI_2-intercalate of polycrystalline Bi2212 was easily obtained by heating at 240 °C for 4 hours with two hours intermittent heat treatment at 190 °C for the pre-intercalation of iodine, the intercalation of HgI_2 into (Bi,Pb)2223 could not be realized simply by reacting the pristine host using a direct reaction between with host and HgI_2 vapor due to the inelastic nature of the unit block consisting of three CuO_2 layers of (Bi,Pb)2223, which is significantly thicker than that of Bi2212. It is therefore necessary to preintercalate iodine molecules into (Bi,Pb)2223 to open the layer lattice, which allows us to obtain the first staged HgI_2 intercalate by subsequent proper open-type intercalation of HgI_2.[13] The organic material can be further intercalated into the HgI_2 intercalated Bi-based superconductor using interlayer complexation.[14]

Preparation of superconducting colloidal particle. Organic intercalated superconductors can be easily dispersed in various organic solvents like DMSO, acetone, and ethanol (EtOH). However, HgI_2 agglomerates and precipitates appeared when the water solvent was mixed with an organic intercalated superconductor. It was also found that the protic solvents like EtOH and methanol may not be appropriate since the superconducting particles suffer from degradation due to the formation proton in solvent. In the case of DMSO, it allows a good dispersion of superconducting colloidal particles, but it is highly viscous and hardly vaporized, and therefore, it is concluded that the DMSO solvent is not appropriate for fabricating membranes by the pressure filtration method. Finally we selected acetone as the most probable solvent, since it can be easily removed after membrane fabrication due to its very low viscosity and relatively low boiling point.[15-16]

Fabrication of membrane. In order to fabricate the superconducting membrane, the pressure filtration method was employed. Since we do not treat superconducting particles at high temperatures, the α-Al_2O_3 membrane was used as a support. Considering the particle size distribution of the superconducting colloidal particles, we were able to select an alumina support with a top layer thickness of 0.2 μm (Inoceramic, German). The organic intercalated superconductor of 2 g was dispersed in acetone and divided into 5 parts of colloidal solution each of around 20 mL. The colloidal solution formed was poured on the plate type support, and finally a vacuum was applied to the filter. After the pore blocking, the resulting membrane was dried in an

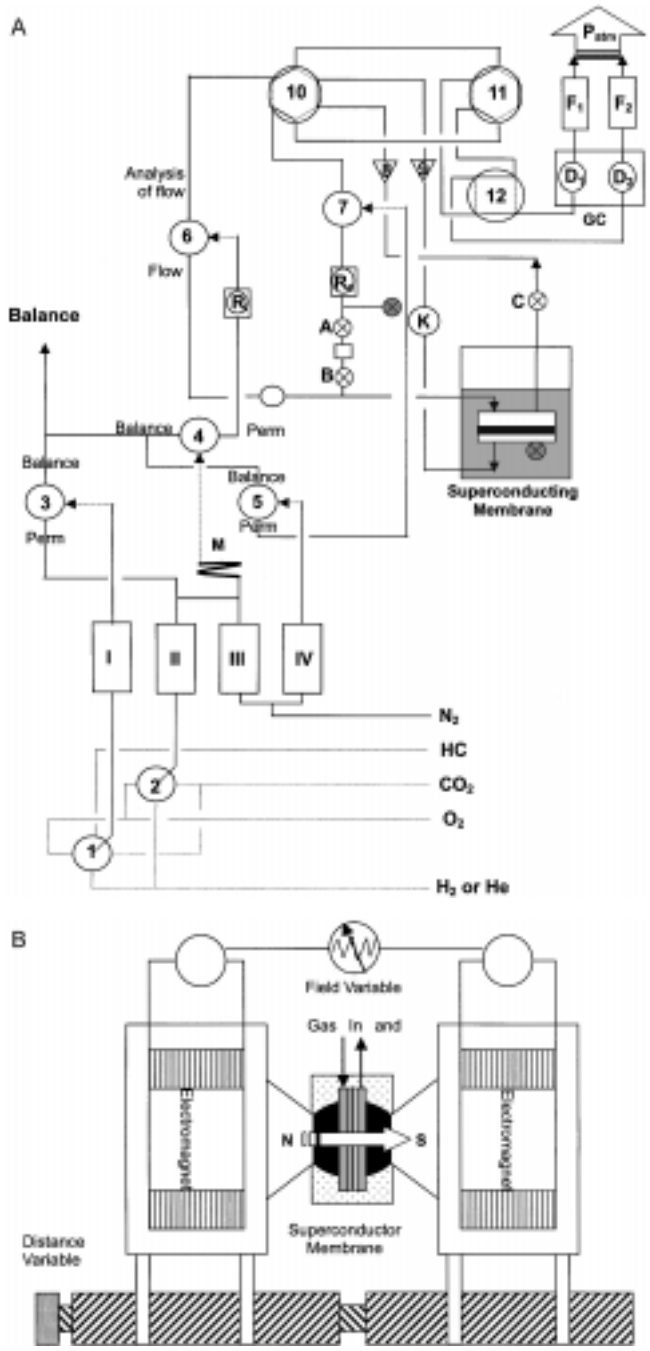

Figure 1. A schematic description of gas separation equipment.

ambient atmosphere.

Characterization. In order to characterize the precursor nanocomposites between the α-Al_2O_3 membrane, superconducting particles and the superconducting porous membrane, powder X-ray diffraction (XRD) analyses (Simens D5000 and INEL CPS120), superconducting critical temperature (T_c) measurements by SQUID, particle size determination by light scattering equipment (Sematec SM200 in ENSCM), morphology observation by scanning electron microscope (SEM, Hitachi S4500 and Leica Spectroscan-260), and pore size analysis by Hg porosimetry (Quantasorb) have been carried out. Gas permeation experiments were

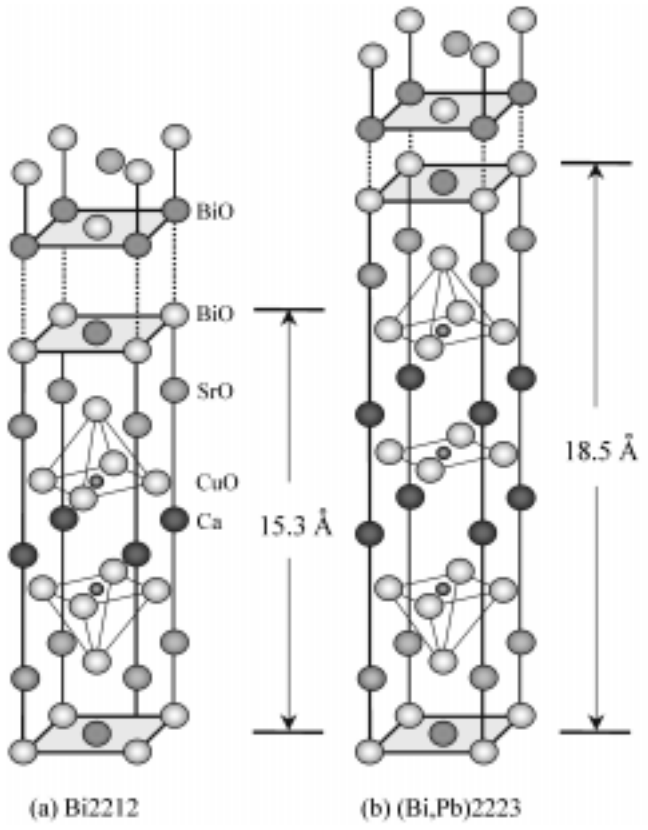

Figure 2. Crystal structures of Bi-based cuprate superconductors, Bi2212(a), (Bi,Pb)2223(b).

performed by using gas permeation equipment as shown in Figure 1A, where N_2 and O_2 gases were mixed with He gas. The composition of each gas was characterized by gas chromatography (HP5890 Series II) with an integrator (HP3396 Series II). A home-made magnetic device was installed as shown in Figure 1B. The applied field is from a few tens of Gauss to a few hundred Gauss after considering the critical magnetic field of the present Bi-superconductor system.

Results and Discussion

Structural description of layered $Bi_2Sr_2Ca_{n-1}Cu_nO_{4+2n}$. Among various high-$T_c$ superconductors, the Bi-based cuprates with a chemical formula of $Bi_2Sr_2Ca_{n-1}Cu_nO_y$ (Bi2201 for $n = 1$; $T_c \approx 10$ K, Bi2212 for $n = 2$; $T_c \approx 85$ K and (Bi,Pb)2223 for $n = 3$; $T_c \approx 110$ K, respectively[17]) are suggested to be the best host compounds candidates for for intercalation reaction, since the Bi_2O_2 layers in these compounds are weakly bound to each other only by the weak van der Waals-type interaction. As shown in Figure 2, these compounds have a mica-like layered structure where the interlayer (Bi-O) bond distance between the Bi_2O_2 layers is 3.7 Å, while the intralayer (Bi-O) bond length is 2.3 Å. Although the other high-T_c superconductors like Tl- and Hg-based superconductors are highly anisotropic in terms of crystal and electronic structure, their out-of-plane bonding

Table 2. Physical properties of various high Tc superconductors for gas separation

Superconductor	Hc_1 (mT)		Hc_2 (T)	T_c (K)	Penetration depth (nm)	
	a,b-axis	*c*-axis			*a,b*-axis	*c*-axis
Bi2201				40		
Bi2212	85		~89	78	270	500
(Bi,Pb)2223		650	~184	110	250	178
YBCO	~25	~90	~120	90	140	~500
Tl2223			~75	125	173	480

Table 3. Powder XRD and T_c results for the superconducting materials

Compounds	*a* (Å)	*c* (Å)	Δc (Å)[a]	T_c (*K*)	ΔT_c (K)[a]
Bi2212	5.40	30.7	–	78	–
HgI_2-Bi2212	5.40	44.9	14.3	68	–10
HgI_2py_2-Bi2212	5.40	52.1	21.4	78	0
(Bi,Pb)2223	5.40	37.1	–	107	–
HgI_2-(Bi,Pb)2223	5.40	51.0	13.9	95	–12
HgI_2py_2-(Bi,Pb)2223	5.40	58.1	21.0	–	–
$C_{12}H_{25}pyHgI_4$-(Bi,Pb)2223	5.40	100.2	63.1	107	0

[a] Difference between pristine Bi-superconductor and intercalates

character is found to be more covalent than their in-plane one, which is in contrast to Bi-based superconductors. The physical properties of various superconductors for gas separation are summarized in Table 2.

Characterization of bi-superconductors and their organic intercalates. The intercalation of organic molecules into the layered superconductor was accomplished *via* the mercuric halide intercalation route because it would be quite difficult to intercalate organic molecules into the superconducting lattice directly due to the severe geometric hindrance of bulky organic molecules. In this respect, a new synthetic method using interlayer complexation reaction was applied to the synthesis of the organic intercalation compounds, (Py-C_nH_{2n+1})HgI_4-$Bi_2Sr_2Ca_{n-1}Cu_nO_y$ and (Py_2HgI_2)-$Bi_2Sr_2Ca_{n-1}Cu_nO_y$, where the bilayers of the pyridinium or pyridine chain are stabilized in-between Bi_2O_2 double layers.[14]

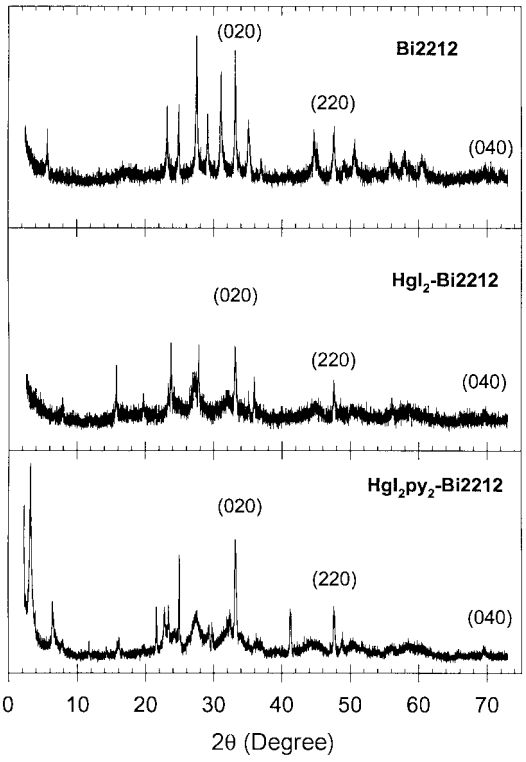

Figure 3. Powder XRD patterns for Bi2212, HgI_2-Bi2212 and pyridine intercalation compound. Note that the first peak, which represents the basal spacing between layers, shifts to the lower angle side while the position of (020), (040), and (220) peaks due to the in-plane component upon HgI_2 and organic intercalation remains.

Figure 3 shows powder XRD patterns for Bi2212 intercalation compounds. As shown in Figure 3, the *c*-axis unit cell parameter for Bi2212 is 15.3 Å. On the other hand, the lattice expansion along the *c*-axis (Δd) upon intercalation was estimated to be ~7.5 Å for the HgI_2 compound,[18] ~10.7 Å for the Py_2HgI_2 compound, and ~32.1 Å for the (Py-$C_{12}H_{25}$)HgI_4 compound,[14] respectively. This increase in the basal spacing is related to the interlayer distance becoming larger, and therefore, the interaction between superconducting layers is more suppressed than that of the host compound, so that the superconducting colloid can be easily obtained. Such an effect can also be observed in the (Bi,Pb)2223 compound, in particular the alkyl pyridinium intercalation compound, whose basal increment (Δd) is as much as 31.6 Å in the case of $C_{12}H_{25}$-pyridinium (Table 3).

Figure 4A and 4B depict the temperature-dependent DC magnetic susceptibilities for the pristine Bi2212 and

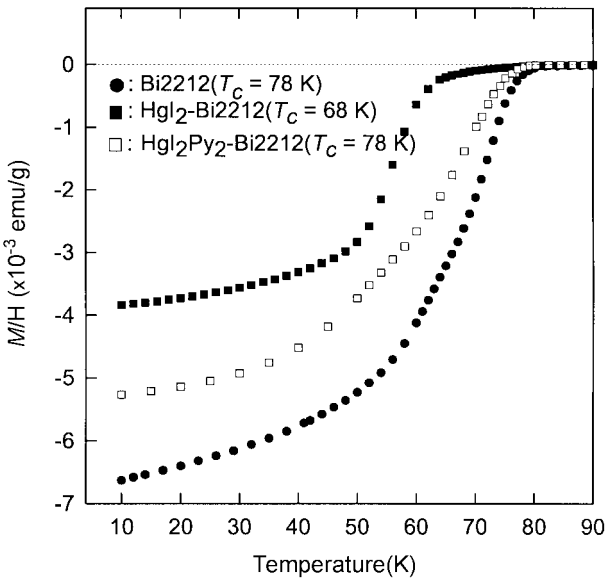

Figure 4. Magnetic susceptibility versus temperature curves for the pristine Bi2212 and its intercalation compounds.

(Bi,Pb)2223 and their intercalation compounds. In spite of extreme lattice expansion upon intercalation of mercuric iodide, all the intercalates still exhibit bulk superconductivity with a slight decrease of superconducting transition temperature (T_c) of about 10 K, compared to the T_c of the corresponding pristine compound. On the other hand, the depressed T_c value upon HgI_2 intercalation is recovered by the organic intercalation, which can be understood as a result of charge restoration of the host block.[14]

Preparation and characterization of superconducting colloidal particles. A superconducting colloid was prepared by superconducting of the organic intercalation compounds in organic solvent, and then by ultrasonicating them for 30 minutes.[15-16] After standing the superconducting colloidal solution for 24 hours in a static condition, the upper part was collected and stored for further treatment. The materials in the lower part turned out to be mainly mercuric iodide intercalates, as confirmed by powder XRD, with a particle size in the range of a few tens of micrometers according to the SEM image.

All the organic intercalation compounds were well dispersed in various organic solvents such as DMSO, DMF, EtOH, and acetone. According to our preliminary experiments, however, aprotic solvents like acetone with low boiling points can be regarded as the best solvents, since they can be removed easily and do not decompose the superconducting phase.

Figures 5A and 5B show the particle size distribution (PSD) for Bi2212 and (Bi,Pb)2223 superconducting colloids in acetone, respectively, obtained by light scattering analysis. The sizes of Bi2212 colloidal particles are distributed from 100 nm to 1 μm with an average of 250 nm and are stable for up to several days. On the other hand, (Bi,Pb)2223 colloidal particles with an average size of 450 nm are even larger than those of Bi2212, which can be understood based on the larger thickness of each repeating unit of (Bi,Pb)2223. One repeating unit of Bi2212 with two Cu-O layers is 15.4 Å, while that of (Bi,Pb)2223 with three Cu-O layers is 18.5 Å as shown in Figure 2.

After drying the superconducting colloids in a vacuum, the resulting powder is determined to be X-ray amorphous,

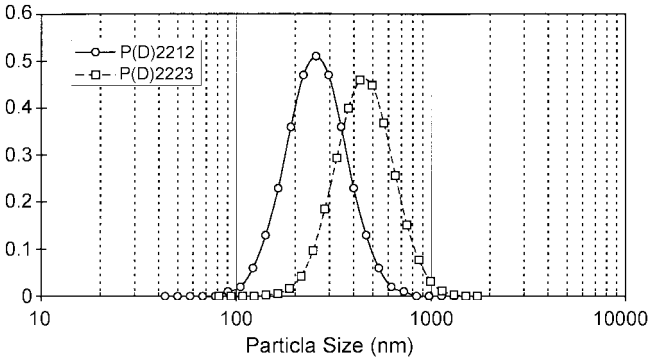

Figure 5. Particle size distribution for Bi2212 and (Bi,Pb)2223 superconducting colloids prepared by pyridinium intercalation route in acetone solvent.

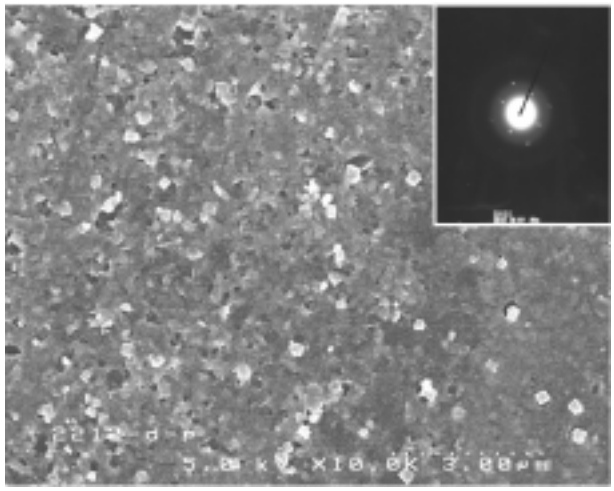

Figure 6. SEM image for Bi2212 superconducting colloidal particles after drying. The inset indicates the selected area electron diffraction pattern.

which means that the exfoliated superconducting colloidal nanosheets are not restacked regularly but assembled randomly with a mosaic structure. This might be the reason why the powder XRD do not show only (00*l*) diffraction peaks upon drying the superconducting colloids, which differs completely from well developed (00*l*) reflection for the restacked organic derivation of layered titanate or α-zirconium phosphates.[19-20]

Figure 6 shows the SEM image for Bi2212 superconducting colloidal particles after drying, and the particle size is highly consistent with the particle size distribution (PSD) result. Even though it is determined to be X-ray amorphous, the superconducting lattice of each particle remains unchanged, as confirmed by the selected area electron diffraction analysis (inset in Figure 6).

The superconducting property for (Bi,Pb)2223 colloidal particles after drying is depicted in Figure 7 together with those for the pristine and the mercuric iodide intercalated (Bi,Pb)2223. Even though the volume fraction is highly diminished, the onset T_c value for superconducting colloidal powder is observed to be almost the same as that for the pristine (Bi,Pb)2223 (inset in Figure 7).

Fabrication and characterization of the superconducting membrane. The superconducting membrane was prepared by filtrating the superconductor colloids through an α-alumina support membrane with a top layer with a pore size of 200 nm.

Figure 8 shows the PSD of the filtrate of superconducting colloid upon repeating the filtration number. The particle size of 250 nm before filtration gradually decreases upon filtration to 120 nm after five filtration rounds. The five successive rounds of filtration were not very effective, resulting in only solvent evaporation, which means that all the pores were blocked by the superconducting colloidal particles. In the case of (Bi,Pb)2223, it is very difficult to obtain pore blocking after five filtration rounds, which may be due to the large particle size.

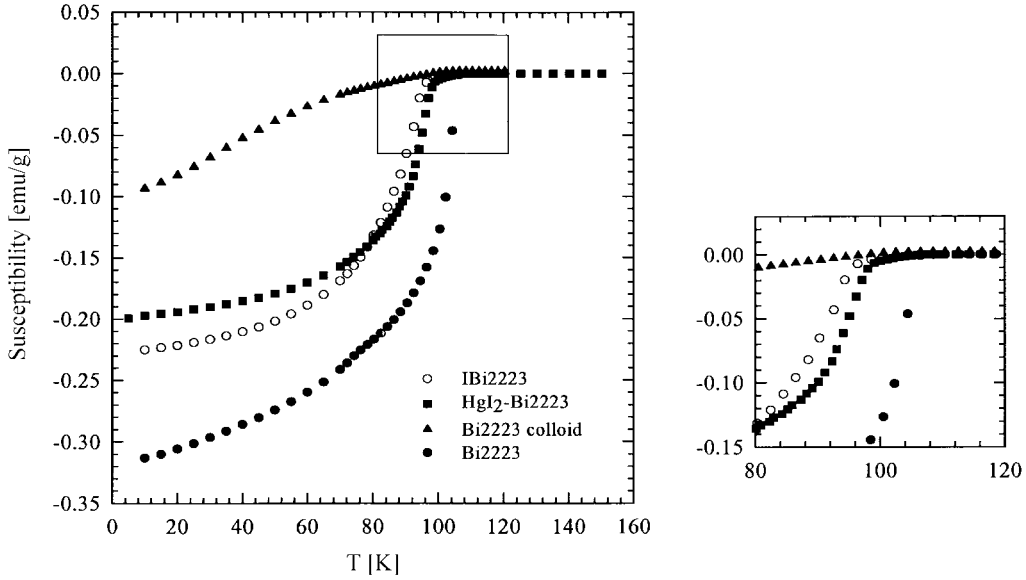

Figure 7. Superconducting properties for (Bi,Pb)2223 superconducting colloidal particles after vacuum drying.

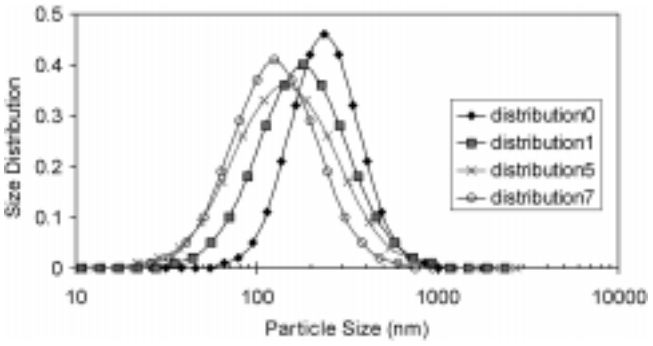

Figure 8. Particle size distribution for the filtrate depending on the number of filtration rounds.

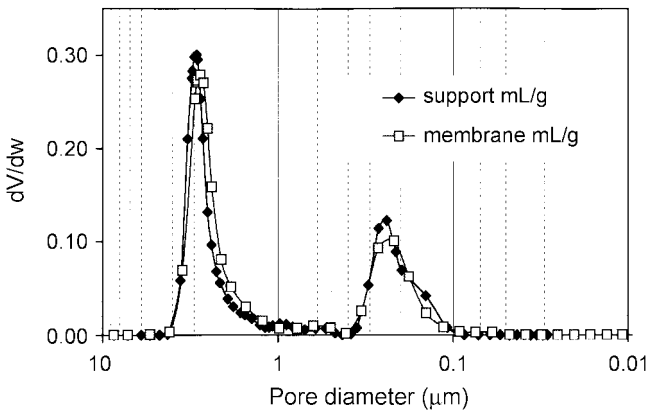

Figure 9. Pore size distribution of superconducting membrane measured by Hg porosimetry.

Figure 9 shows the pore size distributions of the obtained Bi2212 superconducting membrane and the α-alumina support, respectively. The pore size reduction in the superconducting membrane was mainly found in a macropore region of 3 μm compared to the α-alumina support and the disappearance of pores was also detected in the other region. The pore volume was also found to decrease in the entire region.

Figure 10 shows the SEM images for the side view and the top view of the superconducting membrane (A) and the support (B), respectively. As can be clearly seen, the superconducting particles are mainly blocked in the region between the intermediate pore and the 3 μm macropore. The layer thickness of superconducting particles was evaluated to be about 40 μm. In the region of the top layer (pore size of 200 nm), we can hardly observe superconducting particles, as shown in Figure 10C. Such a positional accumulation and quantity of superconducting particles can certainly be distinguishable, as can be observed in Figure 10D, which represents the side and top views of the Bi2212 superconducting membrane measured by a backscattering image mode where the white spots represent heavy metal atoms like Bi, Cu, Sr *etc.* comprising the superconducting lattice.

Figures 11 and 12 show a closer view of the region blocked by superconducting particles. One can see plate-like particles with an average size of 250 nm which are stacked in between the large α-alumina particles (Figure 11A) and perpendicular to the direction of evacuation (Figure 11B). Therefore, it is possible to model the present superconducting membrane as shown in Figure 12.

Gas permeation experiment. The gas seperation experiments were carried out for the obtained Bi2212 and (Bi,Pb)2223 superconducting membranes by using a device as shown in Figure 1. All the experiments were performed at room temperature and at liquid nitrogen temperature, respectively. The initial and final gas compositions before and after permeation were determined by gas chromatograpy. A helium mixture gas containing about 10% of each gas in composition was used for permeation experiments upon consideration of the boiling points of O_2(73 K) and N_2(62) K.[21]

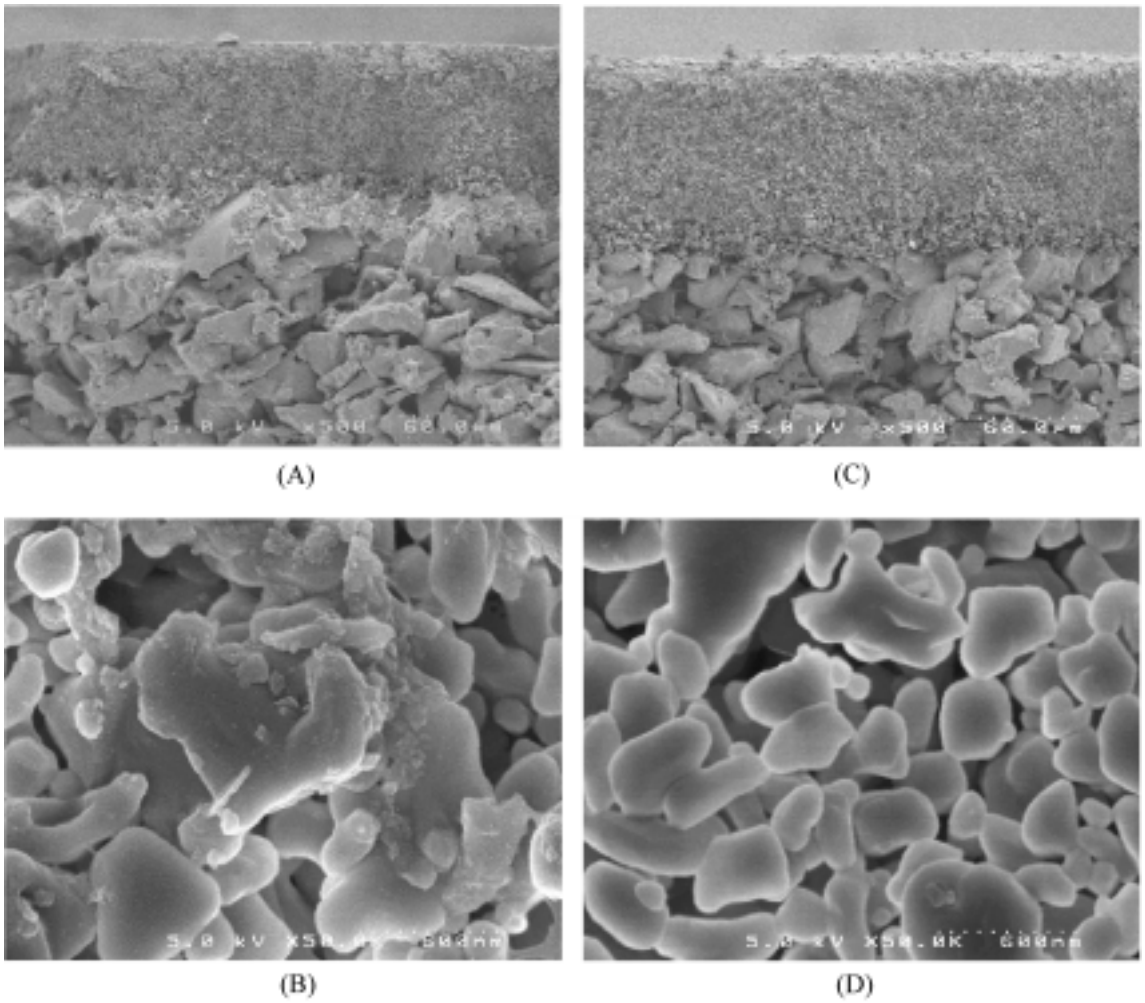

Figure 10. SEM images for the (Bi,Pb)2223 superconducting membrane [(A) side view and (B) top view] and SEM images for the support a-alumina membrane [(C) side view and (D) top view].

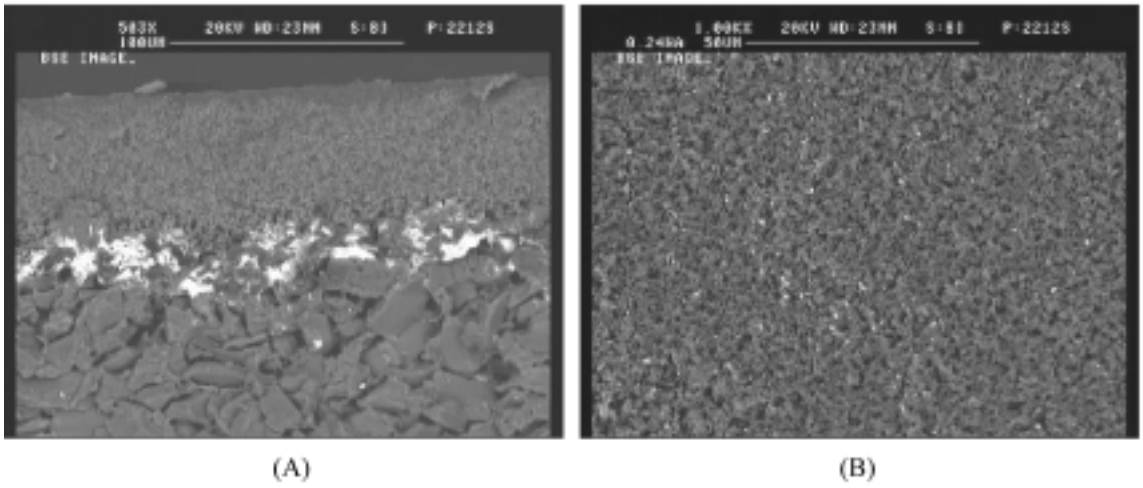

Figure 11. Back-scattering SEM images for the Bi2212 superconducting membrane. (A) side view and (B) top view.

As shown in Table 4, no significant permeation difference between diamagnetic nitrogen and paramagnetic oxygen could be observed for any of the superconducting membranes. For all the gas mixtures, it was confirmed that the Meissner effect does not markedly influence the gas separation, which is in good agreement with a previous result on the YBCO superconducting filter.[10] Only the nitrogen permeation is slightly decreased from 2.6×10^{-7} mol/sec Pa m^2 for the

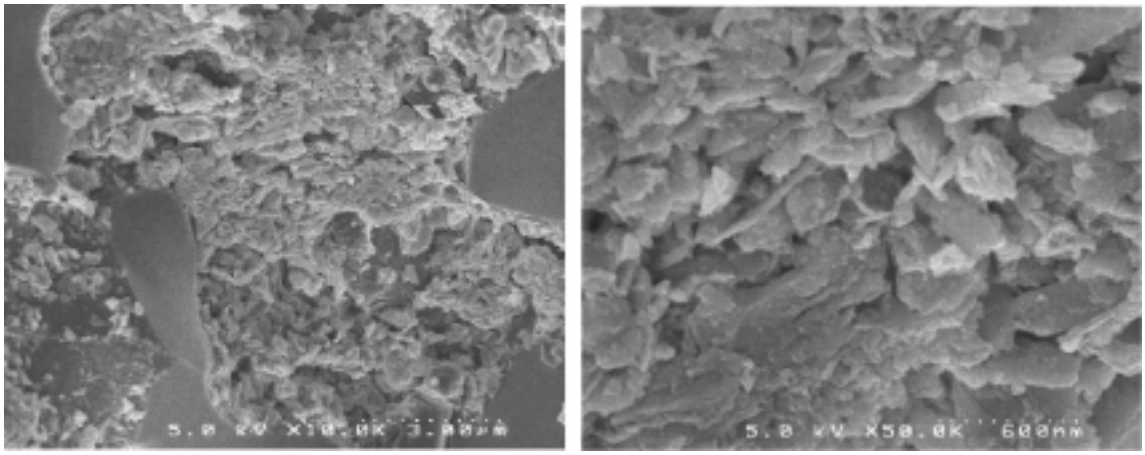

Figure 12. SEM image for the Bi2212 superconducting membrane (closer view in pore blocking region).

Table 4. Gas permeation results for the (Bi,Pb)2223 superconducting membrane

N_2 RT	non magnetic	800G	1100G	1500G	O_2 RT	non magnetic	800G	1100G	1500G
P_0(Pa)[a]	100000	100000	100000	100000	P_0(Pa)[a]	99950	99950	99950	99950
T(°C)	26.0	26.0	26.0	26.0	T(°C)	26.5	26.5	26.7	26.7
T(K)	299.15	299.15	299.15	299.15	T(K)	299.65	299.65	299.85	299.85
ΔP_e(Pa)[b]	18600	18700	18700	18700	ΔP_e(Pa)[b]	18350	18250	18250	18250
C_e(%)[c]	9.4	9.5	9.5	9.6	Ce(%)[c]	8.6	8.6	8.6	8.6
ΔP_i(Pa)[b]	18600	18700	18700	18700	ΔP_i(Pa)[b]	18250	18350	18350	18450
C_I(%)[d]	9.6	9.8	9.8	9.9	C_I(%)[d]	9.0	9.0	9.0	9.0
F(Ci/Ce)[e]	1.02	1.03	1.03	1.03	F(Ci/Ce)[e]	1.05	1.05	1.05	1.05
					$\alpha(N_2/O_2)$[f]	0.98	0.99	0.99	0.99
N_2 LT	non magnetic	800G	1100G	1500G	O_2 LT	non magnetic	800G	1100G	1500G
P_0(Pa)[a]	101400	101400	101400	101400	P_0(Pa)[a]	101400	101400	101400	101400
T(°C)	26.5	26.5	26.5	26.5	T(°C)	26.5	26.2	26.2	26.2
T(K)	299.65	299.65	299.65	299.65	T(K)	299.65	299.35	299.35	299.35
ΔP_e(Pa)[b]	16500	16500	16500	16500	ΔP_e(Pa)[b]	16900	16900	17000	17000
C_e(%)[c]	7.9	7.9	7.9	7.9	Ce(%)[c]	8.9	8.9	8.8	8.9
ΔP_i(Pa)[b]	16500	16500	16600	16500	ΔP_i(Pa)[b]	17000	17000	17000	17100
C_I(%)[d]	8.9	8.8	8.9	8.9	C_I(%)[d]	9.8	9.8	9.8	9.8
F(Ci/Ce)[e]	1.13	1.11	1.13	1.13	F(Ci/Ce)[e]	1.10	1.10	1.11	1.10
					$\alpha(N_2/O_2)$[f]	1.02	1.01	1.01	1.02

[a] pressure of outlet, [b] pressure difference, [c] the concentration of nitrogen or oxygen with helium in feed gas, [d] the concentration of nitrogen or oxygen with helium in permeated gas, [e] F(Ci/Ce) = the rate of permeated gas *vs.* feed gas, [f] $\alpha(N_2/O_2)$ = the rate of $F(N_2)$ *vs.* $F(O_2)$.

alumina support to 2.4×10^{-7} mol/sec Pa m^2 for the superconducting membrane due to the pore packing by superconducting particles.

In order to investigate the effect of the magnetic field on the separation of paramagnetic oxygen and diamagnetic nitrogen, gas permeation experiments were carried out under magnetic fields of 800 G~1500 G with a home-made electromagnetic device.

However, we found that the magnetic field alone does not have any effect on the gas separation for the present membranes. The main reason for this is thought to be the size of the superconducting particles and the superconducting property of the present membrane. Under the applied magnetic field, one should consider the pore size and magnetic field strength.[11] According to our previous theory, a particle size of 250 nm was thought to be too small compared to the penetration depth of the (Bi,Pb)2223 superconductor, where the magnetic flux penetrates the superconducting particles and, as a consequence, the effective magnetic field could not be concentrated to the pore. The best solution to achieve a good selectivity is to make the superconducting particles become mutually interconnected by heat treatment. However, the present α-alumina support is rather reactive with some element in the present Bi-cuprate superconductor.[22] In order to solve such problems, we are now currently proceeding to investigate a new porous support based on magnesia or yttria-stabilized zirconia (YSZ).

Summary

In the present study, the Bi2212 and (Bi,Pb)2223 superconducting colloidal particles could be obtained by using an organic intercalation route, and their structural and magnetic properties have been studied in detail. Simultaneously, we were able to demonstrate for the first time how to prepare the Bi2212 and (Bi,Pb)2223 superconducting membranes by the filtration method, and could characterize membrane properties by powder XRD, SEM, and mercury porosimetry. Permeation experiments were also conducted for the superconducting membranes for applying them to the gas separation between diamagnetic and paramagnetic molecules based on the Meissner effect. Although no significant permeation difference between nitrogen and oxygen for any superconducting membrane could be observed with or without magnetic fields, we found that the nitrogen permeation is slightly reduced from 2.6×10^{-7} mol/sec pa m^2 for the alumina support to 2.4×10^{-7} mol/sec pa m^2 for the present membrane as a result of the pore packing due to the superconducting particles.

Acknowledgment. This work was in part supported by KOSEF (Korea Science and Engineering Foundation), SIC (Support of International Cooperation; project number 305-1990024-1), CSCMR (Center for Strongly Correlated Materials Research), and by a NRL (National Research Laboratory) program. We thank Dr. Jose Sanchez, Dr. J. Portier, Dr. F. Grasset, and Mr. S.-J. Kim for their helpful assistance and discussions.

References

1. Cot, L. *Fundamentals of Inorganic Membrane Science and Technology*; Burggraaf, A. J., Ed.; Elsevier (NL): 1996: Chap 1.
2. *CRC handbook of Chemistry and Physics*, 64th ed; 1984; F-45.
3. Parthasarathy, R. V.; Menon, V. P.; Martin, C. R. *Chem. Mater.* **1997**, *9*, 560.
4. Baker, R. W. *Membrane Technology and Applications*; McGraw-Hill: New York, 2000.
5. Chen, C. S.; Xie, W. L. S.; Zhang, G. G.; Liu, H.; Meng, G. Y. ; Peng, D. K. *Adv. Mater.* **2000**, *12*, 1132.
6. Cheng, L. S.; Yang, R. T. *Ind. Eng. Chem. Res.* **1995**, *34*, 2021.
7. Reich, S.; Cabasso, I. *Nature* **1989**, *338*, 330.
8. Yoon, J. B.; Ayral, A.; Cot, L.; Choy, J. H. *Bull. Korean Chem. Soc.*, to be submitted in 2001.
9. Yamamoto, A.; Ishizu, T.; Ichihara, K. *US patent*, US4704139, 1987.
10. Sawai, Y.; Bamba, N.; Ishizaki, K.; Hayashi, S. *J. Porous Mater.* **1995**, *2*, 151.
11. Sawai, Y. *Ph.D. Thesis*; Nagaoka University of Technology: 1994.
12. Sawai, Y.; Ishizaki, K.; Hayashi, S.; Jain, R. *Porous Materials*, *Ceramic Transactions*; Ishizaki, K., Sheppard, L., Okada, S., Hamasaki, M., Huybrechts, B., Eds.; Am. Ceram. Soc.*:* Westerville, Ohio, 1993; Vol. 31, p 335.
13. Hwang, S. J. *Ph.D. Thesis*; Seoul National University: Seoul, 1998.
14. Choy, J. H.; Kwon, S. J.; Park, G. S. *Science* **1998**, *280*, 1589.
15. Choy, J. H.; Lee, W.; Jang, E. S.; Kwon, S. J.; Hwang, S. J.; Kim, Y. I. *Mol. Cryst. & Liq. Cryst.* **2000**, *341*, 4479.
16. Choy, J. H.; Kwon, S. J.; Hwang, S. J.; Jang, E. S. *MRS Bulletin* **2000**, *25*(9), 32.
17. Tarascon, J. M.; McKinnon, W. R.; Barbaoux, P.; Hwang, D. M.; Bagley, B. G.; Greene, L. H.; Hull, G. W.; LePage, Y.; Stoffel, N.; Giroud, M. *Phys. Rev. B* **1988**, *38*, 8885.
18. Choy, J. H.; Hwang, S. J.; Park, N. G. *J. Am. Chem. Soc.* **1997**, *119*, 1624.
19. Kaschak, D. M.; Johnson, S. A.; Hooks, D. E.; Kim, H. N.; Ward, M. D.; Mallouk, T. E. *J. Am. Chem. Soc.* **1998**, *120*, 10887.
20. Abe, R.; Shinohara, K.; Tanaka, A.; Hara, M.; Kondo, J. N.; Domen, K. *Chem. Mater.* **1998**, *10*, 329.
21. *CRC Handbook of Chemistry and Physics*, 64th ed; 1984; p D-213.
22. Gorette, K. C.; Cuber, M. M.; Feng, L. R.; Fisher, B. L.; Jiang, M.; Lanagan, M. T.; Balachandran, U.; Xu, Y.; Xu, M. *IEEE Transactions on Applied Superconductivity* **1999**, *9*, 1896.